Extensively Reducing Interfacial Resistance by Ultrathin Pt Layer between Garnet-type Solid-state-electrolyte and Li-metal Anode

Yu-Kai Liao[†], Zizheng Tong[‡], Chia-Chen Fang[||], Shih-Chieh Liao[||], Jin-Ming Chen[||], Ru-Shi Liu*[,‡] and Shu-Fen Hu*[,†]

[†]Department of Physics, National Taiwan Normal University, Taipei 116, Taiwan

[‡]Department of Chemistry, National Taiwan University, Taipei 106, Taiwan

[||]Material and Chemical Research Laboratories, Industrial Technology Research Institute, Hsinchu 300, Taiwan.

* Corresponding authors

Correspondence and requests for materials should be addressed to Shu-Fen Hu (email: sfhu.hu@ntnu.edu.tw), Ru-Shi Liu (email: rsliu@ntu.edu.tw)

Figure captions

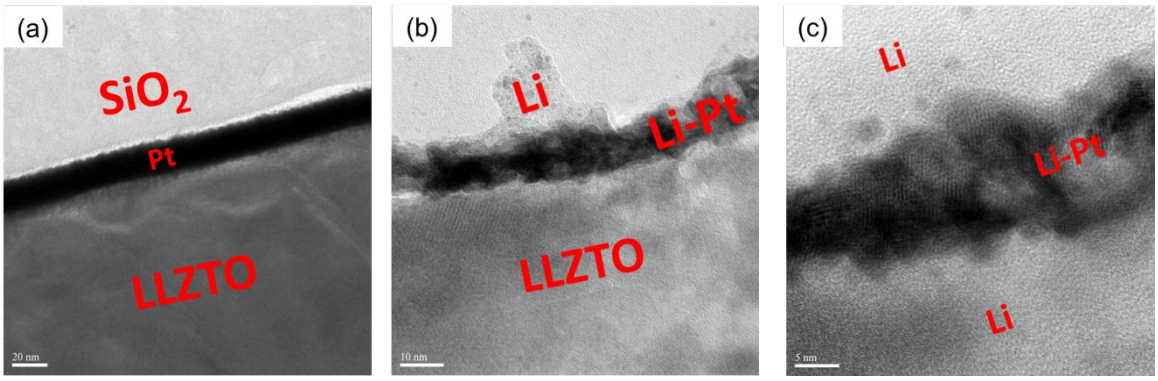

Figure S1. Typical cross-section transmission electron microscope image of (a) SiO_2/Pt/LLZTO, where SiO_2 was used as a protective layer to avoid the influence of FIB Pt sputtering. (b) Li-Pt alloy interface between Li and LLZTO and 3D diffusion of (c) Li/Li-Pt/Li, which is in the Li layer.

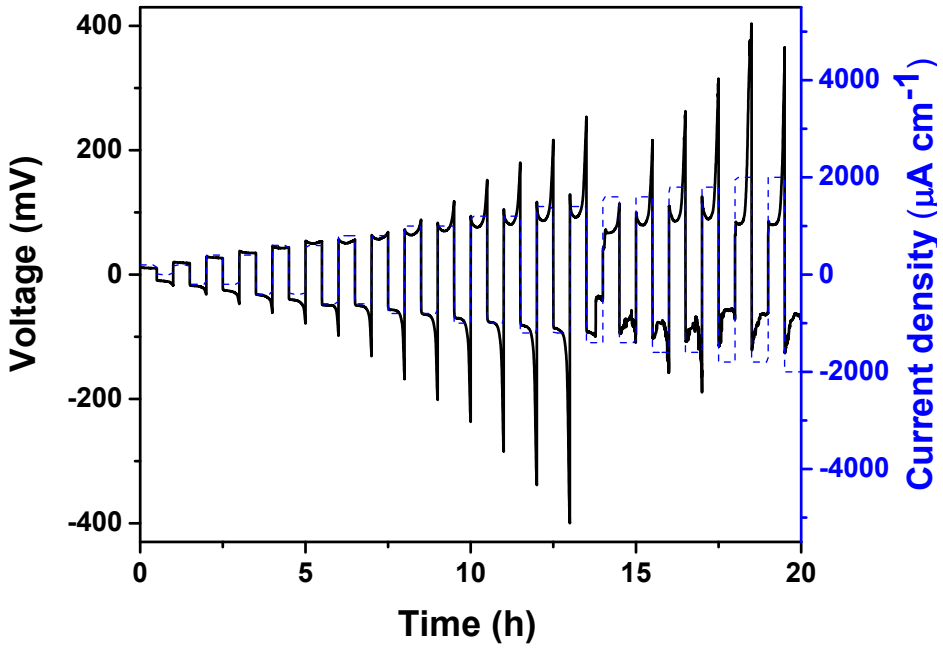

Figure S2. Critical current density of Li-Pt | LLZTO | Li-Pt cell under step-increased current densities with a set from 0.2 mA cm^{-2} to 2 mA cm^{-2}.

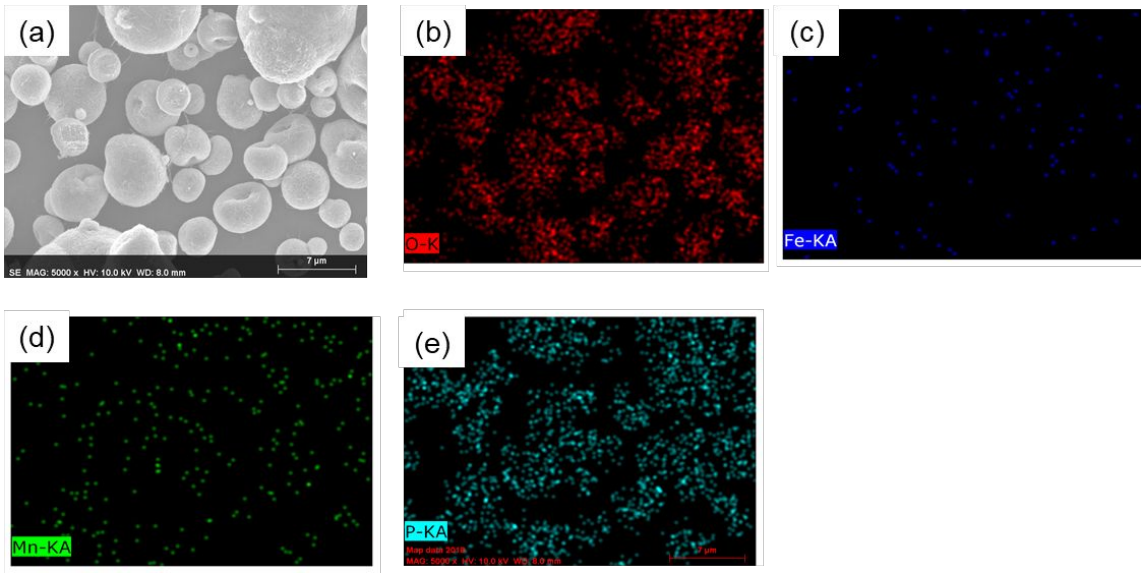

revised Figure S3. SEM image and corresponding EDX mapping. (a) Powders of cathode material LMFP. EDX mapping images of (b) O, (c) Fe, (d) Mn, and (e) P elements. (f) Particle-size analysis of LMFP powders.

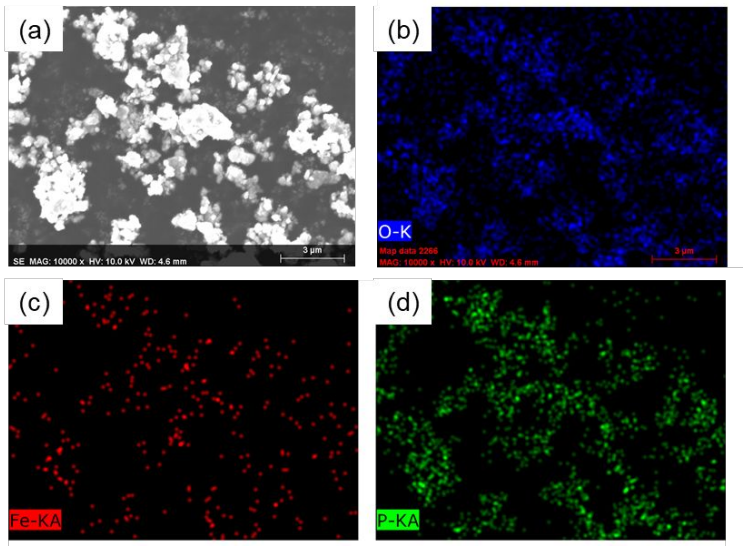

Figure S4. SEM image and corresponding EDX mapping. (a) Powders of cathode material LMFP. EDX mapping images of (b) O, (c) Fe, and (d) P elements.

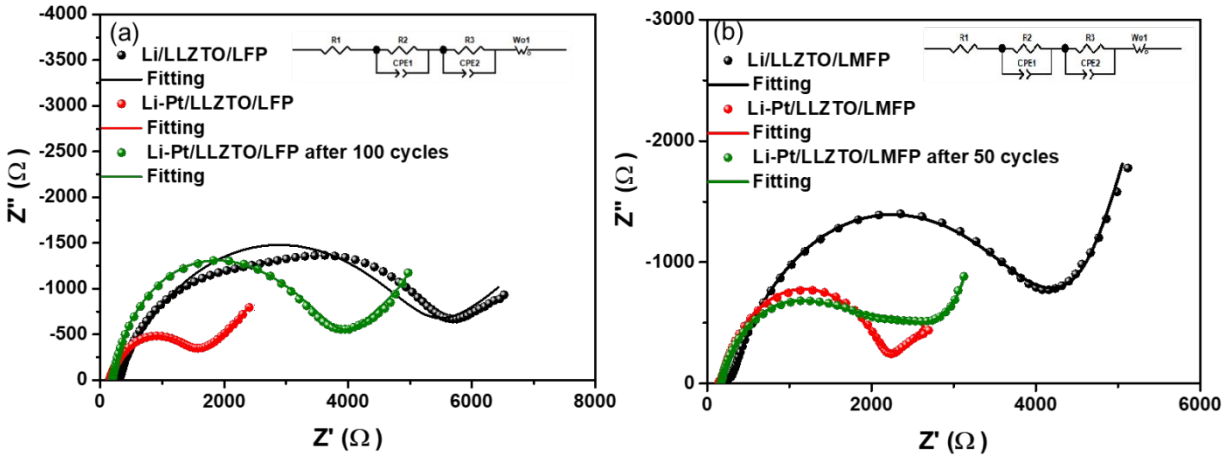

Figure S5. AC impedance plot of full cells with and without thin Pt film modified. (a) cathode as LFP and (b) cathode as LMFP.

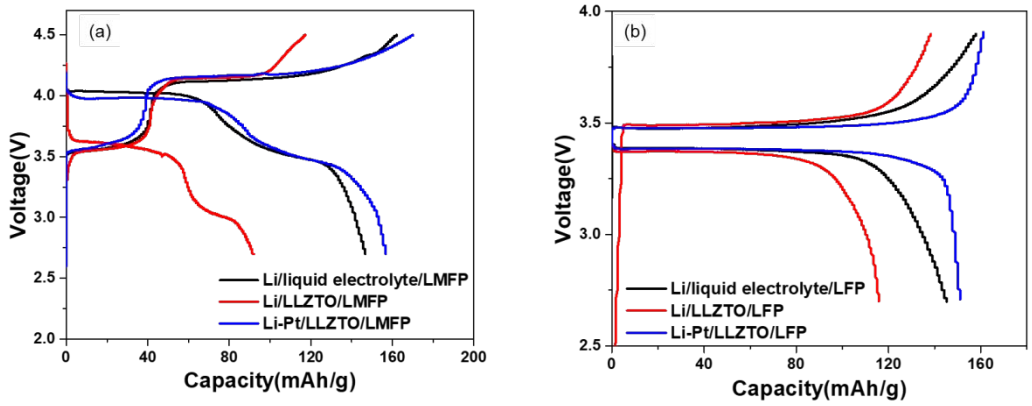

Figure S6. Galvanostatic first charge–discharge curves with (a) LMFP cathode and (b) LFP cathode.

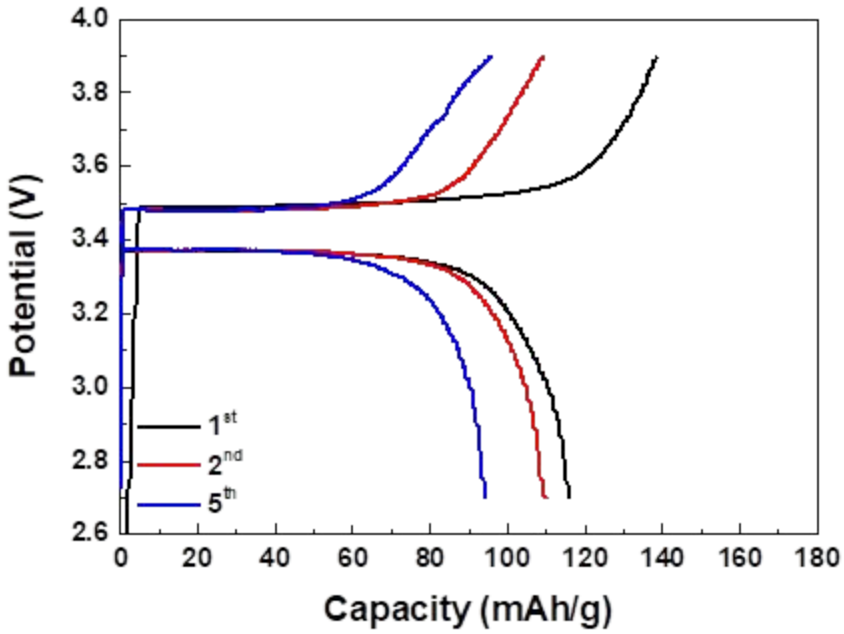

Figure S7. Galvanostatic charge–discharge curves of Li/LLZTO/LFP at room temperature and 0.1 C.

Table S1. Comparison of the interface modification with previous works.

Material	Si	Ge	Al	Mg	Sn	Sn	Graphite	Au	Pt
Method	PE-CVD	E-beam evaporator	E-beam evaporator	Sputtering	Co-melted	sputtering	Draw by pencil	sputtering	sputtering
Thickness (nm)	~10	20	20	5, 10, and 100	N/A	10	N/A	80	20
R_{int} (Ω cm^2)	127	115	75	70	7	46	105	95	9
Reference	1	2	3	4	5	6	7	8	This work

References

(1) Luo, W.; Gong, Y.; Zhu, Y.; Fu, K. K.; Dai, J.; Lacey, S. D.; Wang, C.; Liu, B.; Han, X.; Mo, Y. Transition from superlithiophobicity to superlithiophilicity of garnet solid-state electrolyte. *J. Am. Chem. Soc.* **2016,** *138*, 12258−12262.

(2) Luo, W.; Gong, Y.; Zhu, Y.; Li, Y.; Yao, Y.; Zhang, Y.; Fu, K.; Pastel, G.; Lin, C. F.; Mo, Y. Reducing interfacial resistance between garnet - structured solid - state electrolyte and Li - metal anode by a germanium layer. *Adv. Mater.* **2017,** *29*, 1606042.

(3) Fu, K. K.; Gong, Y.; Liu, B.; Zhu, Y.; Xu, S.; Yao, Y.; Luo, W.; Wang, C.; Lacey, S. D.; Dai, J. Toward garnet electrolyte–based Li metal batteries: An ultrathin, highly effective, artificial solid-state electrolyte/metallic Li interface. *Sci. Adv.* **2017,** *3*, e1601659.

(4) Fu, K.; Gong, Y.; Fu, Z.; Xie, H.; Yao, Y.; Liu, B.; Carter, M.; Wachsman, E.; Hu, L. Transient behavior of the metal interface in lithium metal–garnet batteries. *Angew. Chem. Int. Ed.* **2017,** *56*, 14942−14947.

(5) Wang, C.; Xie, H.; Zhang, L.; Gong, Y.; Pastel, G.; Dai, J.; Liu, B.; Wachsman, E. D.; Hu, L. Universal soldering of lithium and sodium alloys on various substrates for batteries. *Adv. Energ. Mater.* **2018,** *8*, 1701963.

(6) He, M.; Cui, Z.; Chen, C.; Li, Y.; Guo, X. Formation of self-limited, stable and conductive interfaces between garnet electrolytes and lithium anodes for reversible lithium cycling in solid-state batteries. *J. Mater. Chem. A* **2018,** *6*, 11463−11470.

(7) Shao, Y.; Wang, H.; Gong, Z.; Wang, D.; Zheng, B.; Zhu, J.; Lu, Y.; Hu, Y.-S.; Guo, X.; Li, H. Drawing a soft interface: an effective interfacial modification strategy for garnet-type solid-state Li batteries. *ACS Energy Lett.* **2018,** *3*, 1212−1218.

(8) Koshikawa, H.; Matsuda, S.; Kamiya, K.; Miyayama, M.; Kubo, Y.; Uosaki, K.; Hashimoto, K.; Nakanishi, S. Electrochemical impedance analysis of the Li/Au-$Li_7La_3Zr_2O_{12}$ interface during Li dissolution/deposition cycles: Effect of pre-coating $Li_7La_3Zr_2O_{12}$ with Au. *J. Electroanal. Chem.* **2019,** *835*, 143−149.